Organic Rankine cycle modelling and the ORCmKit library: analysis of R1234ze(Z) as drop-in replacement of R245fa for low-grade waste heat recovery

Davide Ziviani[a,], Rémi Dickes[b], Sylvain Quoilin[b], Vincent Lemort[b],
Michel De Paepe[a], Martijn van den Broek[a]*

[a] *Department of Flow, Heat and Combustion Mechanics, Ghent University, Ghent, Belgium,*
davide.ziviani@ugent.be, Michel.DePaepe@ugent.be, martijn.vandenBroek@ugent.be
[b] *Department of Mechanical and Aerospace Engineering University of Liege, Liege, Belgium,*
rdickes@ulg.ac.be, squoilin@ulg.ac.be , Vincent.lemort@ulg.ac.be
[*] *corresponding author*

Abstract:

Due to the wide interest in organic Rankine cycles (ORCs) as a sustainable technology and the importance of numerical analyses and optimization procedures while considering such systems, we created a dedicated open-source library named "ORC modelling Kit" (ORCmKit). The comprehensive library includes single components and overall models for subcritical, transcritical and supercritical ORCs. Three main programming environments are currently supported: Matlab, Python and EES (Engineering Equation Solver). A detailed steady-state cycle model of a small-scale regenerative ORC with a single-screw expander is used to evaluate the performance influence of R1234ze(Z) as a drop-in replacement of R245fa currently used in the installation. The ORC system is used to recover low-grade waste heat with a temperature range between 90°C and 120°C. A thermal oil heater is used to simulate the heat source. A parametric study is carried out to investigate the performance of the system throughout the range of interest in order to optimize the ORC with R1234ze(Z).

Keywords:

ORCmKit, open-source, waste heat recovery, low-GWP refrigerants, ORC.

1. Introduction

Nowadays, it is well known that ORCs (Organic Rankine Cycles) represent a viable solution to recover waste heat from industrial processes as well as to convert renewable energy sources such as solar, geothermal and biomass into electric power [1].
Numerical and experimental studies have been carried out to optimize such systems. Working fluid screening (either pure components or mixtures) [2], cycle architecture [3] and component sizing and selection [4-5] are the main research lines related to ORCs, together with thermo-economic aspects [6].
Recently, the discussion on a possible amendment to the Montreal Protocol on substances that deplete the ozone layer, could lead to gradually phase down the consumption and the production of hydrochlorofluorocarbons (HCFCs) and hydrofluorocarbons (HFCs) and to replace them with new low-GWP (Global Warming Potential) working fluids, referred to as hydrofluoroolefins (HFOs) or fourth generation refrigerants [7-8]. As outlined by Petr and Raabe [9], many commercial ORC, installations run with R245fa which has high GWP and long atmospheric lifetimes. Hence, it is important to assess potential drop-in replacements for HFCs and study their impact on the system performance. As a further step, ORC systems could potentially be optimized to run with HFOs and hydrochlorofluoolefins (HCFOs).

As HFOs such as R1234yf and R1234ze(E) have started to be used in commercial applications for vapour compression technologies replacing R134a [10-11], the potential of HFOs and HCFOs in ORC applications gained interest. Le et al. [12] optimized a baseline (non-regenerative) and regenerative supercritical ORCs for a low-temperature heat source fixed at 150°C. R1234yf and R1234ze(E) were considered as HFOs. The maximum electrical power was found with R1234ze(E). Among optimal low-GWPs, R32 and R152 showed the best system efficiency. Datla and Brasz [13] investigated R1233zd(E) as an alternative for R245fa in an existing 75 kW oil-free low-temperature ORC system with a radial turbine. They concluded that the lower saturation pressure and vapour density of R1233zd(E) led to a 7% increase of the shaft power and an 8.7% higher cycle efficiency without major effects on turbine design and consequently, the ratio cost/kW decreased for the existing R245fa machine. A new developmental hydrofluoroolefin R1336mzz(Z), originally referred to as DR-2, was recently disclosed as a potential working fluid for ORCs. Kontomaris K.K. [14] presented the thermo-physical properties and safety and environmental characteristics. The relatively high critical temperature, high thermal stability and low vapour pressure represent suitable characteristics for ORC applications. For example, in the case of an ORC with a regenerator operating between 25°C and 160°C, the net cycle efficiency could be as high as 25%. R1336mzz(Z) represents a candidate to replace R245fa. However, the thermo-physical properties are not available yet for the general public. Petr and Raabe [9] numerically evaluated R1234ze(Z) as drop-in replacement for R245fa for both subcritical and transcritical ORC applications (heat sources in the range of 100°C up to 250°C), using a simplified cycle model without accounting for the geometry and performance of real components. They concluded that for temperatures above 224°C, R1234ze(Z) showed a slightly higher net power but for the majority of the range of heat source temperatures considered, the performance was in line with R245fa.

In this paper, the potential of R1234ze(Z) to replace R245fa as working fluid has been investigated in an existing regenerative sub-critical ORC with an 11 kWe single-screw expander. A comparison with another suitable candidate as drop-in replacement for R245fa, R1233zd(E), is also proposed. A detailed cycle model that includes the characteristics of each component is used to carry out the numerical simulations. The model has been previously validated with a set of 20 steady-state experimental points [15]. The cycle model developed is part of an open-source library dedicated to the steady-state simulation and analysis of ORC systems both at component and cycle levels and calibration methodologies for empirical and semi-empirical models. The library, named "ORC modelling Kit" or "ORCmKit"[1] aims to close the lack in the scientific community of open-source tools to study ORCs. The library is described in a greater detail in a companion paper [16]. Three main programming languages are currently supported: Matlab, Python 2.7, and EES (Engineering Equation Solver).

Table 1. Summary of thermos-physical properties [9,13,14], safety and environmental data of the low-GWP working fluids and R245fa.

Fluid	MM (kg kmol^{-1})	T_{crit} (°C)	p_{crit} (kPa)	OEL (ppm)	Safety group	AL (yr)	ODP (-)	GWP 100yr.
R245fa	134.05	153.9[17]	3651.0	300	B1	7.6[8]	0.000	1020
R1234ze(E)	114.04	109.4	3635.3	1000	A2L	0.045[18,19]	0.000	<6
R1234ze(Z)	114.04	153.7	3533.0	800	A2L	0.027-0.049 [20,22]	0.000	<3
R1233zd(E)	130.49	166.5	3623.6	800	A1	0.071[21]	0.000	1
R1336mzz(Z)	164.06	171.3	2900.0	500	A1	0.060[14]	0.000	2

---

[1] ORCmKit library can be accessed on GitHub (https://github.com/orcmkit/ORCmKit) or through KCORC website (http://www.kcorc.org/en/open-source-software/)
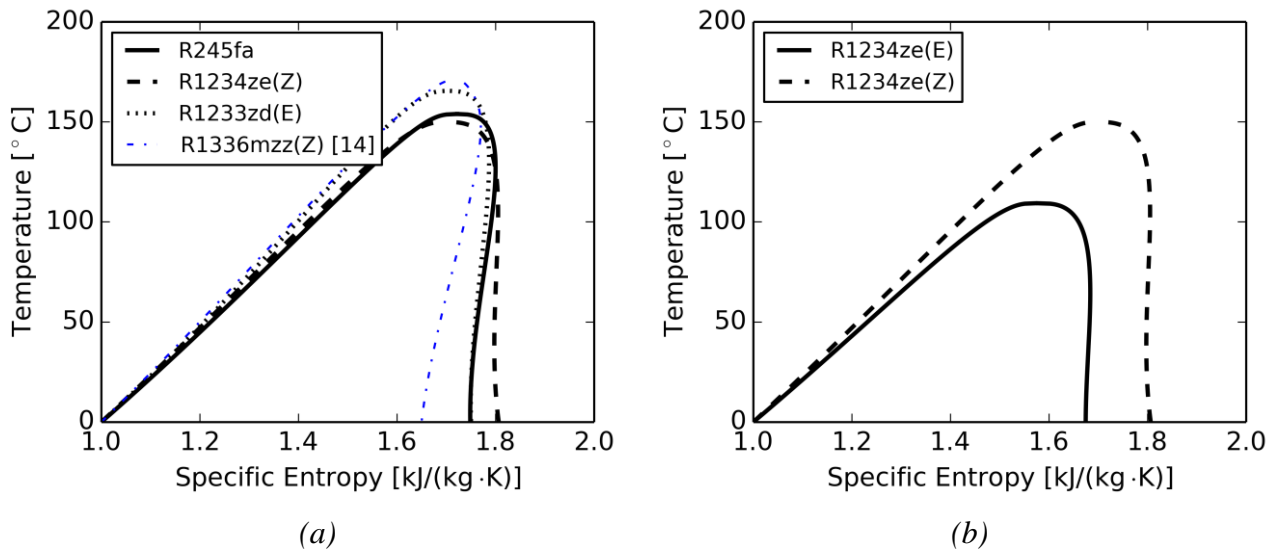
Fig. 1. (a) Comparison of T-s thermodynamic diagrams of R245fa and HFOs R1234ze(Z), R1233zd(E) and R1336mzz(Z). Note that since R1336mzz(Z) is not available in REFPROP 9.1[23], the saturation curves have been obtained qualitatively from Kontomaris K. [14]; (b) Comparison between R1234ze isomers (E) and (Z).
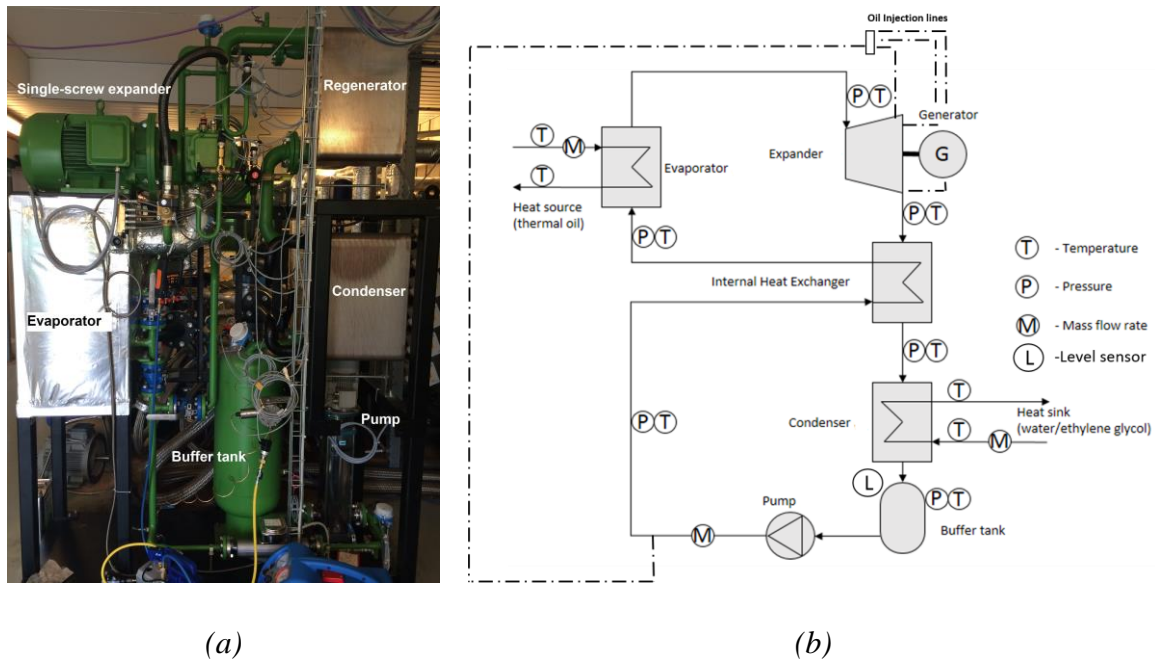

Fig. 2. (a) Regenerative ORC installation with 11 kWe single screw expander; (b) cycle scheme with main components and sensors labelled (b).

2. Low-GWP working fluids and ORC working conditions

2.1. Thermodynamic properties and safety and environmental data

As outlined earlier, low-GWP R1234ze(Z) is investigated as drop-in replacement for R245fa. Additional low-GWP refrigerants are also considered as potential candidates for low-temperature waste heat recovery ORC systems. The candidates taken into consideration are listed in Table 1 along with some thermo-physical properties and safety and environmental data. R1336mmz(Z) shows the highest critical temperature at lower critical pressure leading to a lower pressure range when compared to R245fa. The average atmospheric lifetime of the low-GWPs is less than 30 days which represents a significant improvement over R245fa.
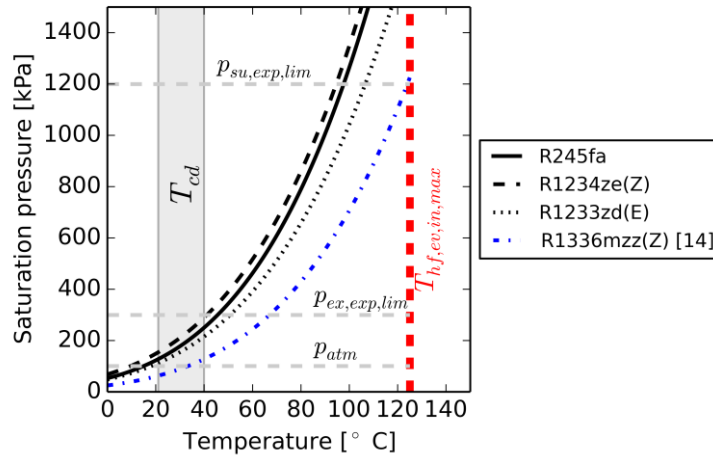
Fig. 3. Saturated curves of the working fluids and the ORC working conditions.

The liquid and vapour saturation curves of the working fluids in the T-s diagrams are shown for comparison in Fig. 1(a). The vapour saturation curves of R245fa and R1233zd(E) show a slight positive slope and they can be regarded as dry-isentropic fluids. R1234ze(Z) is an isentropic working fluid while R1336mzz(Z) is a dry working fluid. As a consequence, all the fluids are suitable for ORC applications.

The 1,3,3,3-tetrafluoropropene (or R1234ze according to ASHRAE standard 34) has two isomers denoted by suffixes (E) and (Z): R1234ze(E) (trans- 1,3,3,3-tetrafluoroprop-1-ene) and R1234ze(Z) (cis-1,3,3,3-tetrafluoroprop-1-ene). The thermo-physical properties of the two isomers are completely different, as can be seen in Fig. 1(b), although both exhibit ultra-low GWPs and short atmospheric lifetime. R1234ze(Z) has a volumetric capacity roughly 50% lower than R1234ze(E) which makes it more suitable as a replacement of R245fa. On the other hand, R1234ze(E) is in line with R134a in terms of operating conditions and applied costs.

The thermo-physical properties have been retrieved from REFPROP 9.1[23]. In the analyses carried out in this paper, only R1234ze(Z) and R1233zd(E) are included since the properties of R1336mzz(Z) are not available yet in the REFPROP database [23]. Additional information can be found in [14].

2.2. Baseline ORC system

The baseline ORC system used as a reference case is an industrial prototype of a subcritical ORC with regenerator, as shown in Fig. 2(a). The system includes a 14-stages centrifugal pump with a vertical axis and a 2.2 kWe motor, three identical plate heat exchangers (PHEX), a liquid receiver and a single-screw expander with an 11 kWe generator connected to an inverter. The piping system is made of steel Temperature and pressure measuring points are located after each component and a Coriolis flow meter is placed after the pump. The electric power output of the expander is measured at the inverter. The shaft power is derived from the generator and inverter performance maps. The working fluid is R245fa with approximately 3%vol. of lubricant oil. The cycle components and the associated thermodynamic states are given in Fig. 2(b). The lubrication of the single-screw expander is ensured by a bleeding line after the working fluid pump. A 250 kW electric heater is used as hot source and Therminol 66 (or T66) is the medium. The cooling medium at the condenser is a mixture of water and ethylene glycol (around 30%vol.). The heat absorbed by the cooling medium is then rejected by means of a roof-top air-cooler. As a consequence, the condensing temperature and pressure in the ORC system are linked to the atmospheric conditions.

The typical operating conditions of the ORC installation are illustrated in Fig. 3. In particular, the hot source temperature is limited at 120°C and the condensing temperature range is between 20°C and 40°C. The atmospheric pressure is indicated as well as the pressure range in which the expander can operate. Originally, the expander was an air compressor and the maximum pressure at the ex-

pander suction side is set at 12 bar, while the pressure at the discharge side is limited to 3 bar. The saturation curves of R245fa and the low-GWP working fluids are drawn on the same figure. It is possible to notice that, for all the working fluids except R1336mzz(Z), the discharge pressure limit is almost reached when the condensing temperature rises above 40°C. This is particularly true for R1234ze(Z). Moreover, R1336mzz(Z) allows lower pressures in the system which can be beneficial especially at higher temperatures without exceeding pressure limitations of components. On the other hand, given the specific working conditions of the present installation, the condensing pressure is sub-atmospheric which may cause non-condensable gases to enter the ORC system in case of leaks.

3. The Organic Rankine Cycle modelling Kit: ORCmKit

3.1. Overview

The design and analysis of ORC systems is accomplished by developing simulation models with different complexity depending on the purpose of the study. Additionally, even though the research on ORCs is gaining interest and the number of papers published is rapidly increasing, there is a lack of knowledge exchange among the ORC community especially regarding advances in modelling techniques. To encourage the sharing of knowledge, researchers from the universities of Ghent and Liege in Belgium created an open-source platform "ORCmKit" dedicated to the steady-state simulation, analysis and optimization of ORC systems. The library supports three programming languages, i.e. Python, EES (Engineering Equation Solver) and Matlab and includes (for each of them) examples of modelling techniques at cycle and components levels as well as calibration methodologies for empirical and semi-empirical models. Both REFPROP and CoolProp routines are used to retrieve the required thermo-physical properties. The ORCmKit library is explained in detail in a companion paper [16]. In this paper, Python is used as programming language to develop the detailed cycle model.

3.2. Detailed ORC cycle model

The cycle model is structured in an object-oriented fashion. Each cycle component is modelled individually as an individual class which allows flexibility when assembling the ORC system considered. Besides the main cycle components (heat exchangers, pump and expander), also the line sets between the component are considered. A simplified model of the liquid receiver is also implemented which is important for the charge estimation. In the following subsections, the cycle model as well as the main component sub-models are briefly introduced. The cycle model requires a set of inputs which are listed in Table 2. The main inputs can be divided in four groups: (i) working fluid selection and rotational speeds of pump and expander; (ii) hot source inlet conditions; (iii) cold sink inlet conditions; (iv) general solution scheme selection. The cycle model formulation includes two solution schemes: either subcooling based solver where the condenser exit subcooling level is fixed and total working fluid charge is estimated, or charge based solver where the total working fluid charge is specified as input and the subcooling level is calculated. In this paper, the subcooling is fixed and the charge is estimated because the aim is to understand the influence of the different drop-in working fluids on the charge required for such system. Ultimately, this will lead to considerations about the cost of the working fluids which is important especially for large installations.

The solution scheme includes a preconditioner which generates two guess values for the evaporating and condensing pressures. The preconditioner can be regarded as a simplified cycle model where only energy balances are used at the evaporator and the condenser. Once the preconditioner converges, the main solver loop starts the iteration process and drives to zero three main residuals: the mass flow rate balance between pump and expander, an overall energy balance of the ORC and the difference between specified and calculated subcooling. Mathematically, the residuals are expressed as:

$$\dot{m}_p - \dot{m}_{\exp} = resid , \qquad (1)$$

$$\dot{W}_p + \dot{Q}_{evap} - \dot{W}_{exp} - \dot{Q}_{cond} = resid, \qquad (2)$$

$$\Delta T_{sub,calc} - \Delta T_{sub,input} = resid. \qquad (3)$$

In addition to the aforementioned residuals, two additional residuals are also computed to ensure the consistency of the simulation. Due to the fact that the regenerator requires inputs both at liquid and at vapour side, pump and expander are solved first and guess values are required for their inlet conditions. Once the pump and the pump discharge line-set are computed, the expander and the expander discharge line set are solved. At this point the regenerator and the exit line sets for liquid and vapour are initialized. Finally, condenser and evaporator and the associated exit line sets are computed. This solution schemes proved to be robust under different conditions. A multi-dimensional solver is used to drive the residuals to zero. In particular, in the Python programming language, the *fsolve* function is used from the *scipy.optimize* module, based on the Powell hybrid method.

3.2.1. Plate heat exchangers

A generalized moving-boundary model has been applied to the three plate heat exchangers (PHEX), the evaporator, the condenser and the regenerator [24]. The PHEX is modelled as a counter flow heat exchanger and after determining the maximum heat transfer rate allowed, the actual heat transfer rate is iterated in order to match the real geometry of the PHEX. Internal pinch points and other non-physical numerical situations are handled by the algorithm by properly expressing the maximum heat transfer rate in each zone. Boiling and condensing heat transfer correlations for the low-GWP working fluids have been obtained from Nagata et al. [25]. The PHEX model also estimates the charge in the heat exchanger which is given as the sum of the charge of each zone (subcooled, two-phase and superheated). The total charge is given by:

$$\text{Charge}_{PHEX} = \sum_{zone} \text{Charge}_{zone} = \sum_{zone} V_{PHEX}\, w_{zone} \bar{\rho}_{zone}, \qquad (4)$$

where V_{PHEX} is the combined volume of all the channels for either the primary or secondary fluid side, $V_{PHEX}\, w_{zone}$ is the volume of a single zone and $\bar{\rho}_{zone}$ is the average fluid density of the zone. The validation of such model has been carried out in [14].

3.2.2. Pump

The performance of the centrifugal pump has been characterized by two empirical correlations. The volumetric flow rate is given as a function of the pressure difference across the pump, Δp_p, and the rotational speed, N_p, by using a fourth order polynomial function:

$$\dot{V}_{r,p} = p_0 + p_1 N_p + p_2 \Delta p_p + p_3 N_p \Delta p_p + p_4 \Delta p_p^2 + p_5 N_p^2 + p_6 N_p^2 \Delta p_p^2. \qquad (5)$$

An alternative formulation with the pump frequency has also been considered. Each term has been normalized with respect to the reference conditions provided by the pump manufacturer.

The isentropic efficiency is related to pressure difference and rotational speed expressed in non-dimensional terms with a set of reference values similar to the previous model for the volumetric flow rate:

$$\varepsilon_{s,p} = f\!\left(\Delta p_p^*, N_p^*\right), \qquad (6)$$

3.2.3. Expander

In order to estimate the performance of the low-GWP working fluids, the single-screw expander has been modelled by introducing two empirical correlations for the isentropic efficiency and the filling factor calibrated on the experimental data of R245fa.

| Variable	Description
PropertyWrapper	Refprop or CoolProp can be selected
Ref	Working fluid string name
HotFluid	Hot source fluid string name
ColdFluid	Cold source fluid string name
$\dot{m}_h, p_{h,su}, T_{h,su}$	Hot source inlet conditions
$\dot{m}_c, p_{c,su}, T_{c,su}$	Cold source inlet conditions
$N_p, N_{\exp}, r_{v,built-in}, V_{g,su}$	Pump and expander data
$(ID, OD, L_{eq})_{lineset}, V_{tot}$	Line sets data and liquid receiver volume
Subcooling_or_charge	Fix the condenser exit subcooling or the total working fluid charge
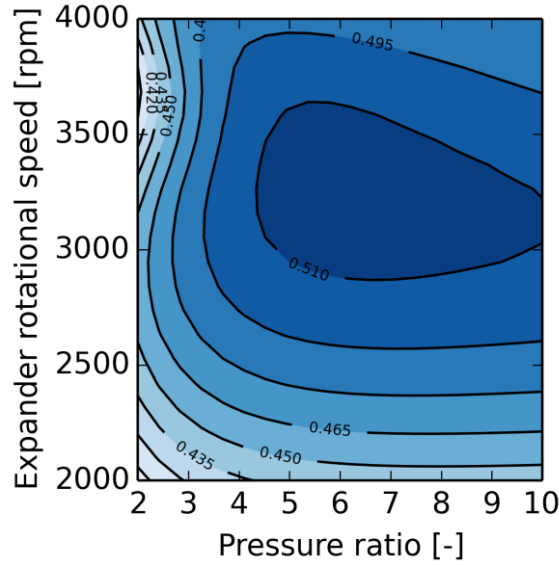
Fig. 4. *Single-screw expander performance map. The contour plot shows the overall isentropic efficiency as a function of expander rotational speed and pressure ratio.*

We assume that the behaviour of the expander does not change if R1234ze(Z) and R1233zd(E) are used as replacements of R245fa. The filling factor is defined as

$$\phi_{FF} = \frac{\dot{m}_r v_{r,\exp,su}(p_{r,\exp,su}, T_{r,\exp,su})}{\dot{V}_{th,\exp}}, \qquad (7)$$

where the theoretical displacement rate of the single-screw expander is given by:

$$\dot{V}_{th,\exp} = 2z_{sr}V_{g,suc}\frac{N_{\exp}}{60}, \qquad (8)$$

where z_{sr} is the number of grooves of the main screw rotor, $V_{g,suc}$ is the chamber volume at suction closure and $N_{\exp}$ is the rotational speed of the expander. The geometrical details of the single-screw expander can be found in Ziviani et al. [26]. The empirical correlation for the filling factor is:

$$\phi_{FF} = k_1 + k_2 \ln\left(\frac{N_{\exp}}{N_{\exp,ref}}\right) + k_3 \left(\frac{p_{ex,\exp}/p_{su,\exp}}{(p_{ex,\exp}/p_{su,\exp})_{ref}}\right) + k_4 \frac{p_{su,\exp}}{p_{su,\exp,ref}}. \qquad (9)$$

The isentropic efficiency model relies on the formulation of the Pacejka equation which has a similar trend to that of the experimental data. The Pacejka equation is suitable to correlate the isentropic efficiency of the volumetric expander with respect either to the specific volume ratio or the pressure

ratio at different rotational speeds. For the sake of compactness only the general form of the equation is reported here. The details of the complete formulation and the calibration procedure can be found in Ziviani et al. [27]. The equation is expressed by:

$$\varepsilon_{oa,\exp} = D \sin\left\{ C \tan^{-1}\left[Bx - E\left(Bx - \tan^{-1}(Bx)\right)\right]\right\}$$

$$E = \frac{Bx_{\max} - \tan\left(\dfrac{\pi}{2C}\right)}{Bx_{\max} - \tan^{-1}(Bx_{\max})} \qquad , (10)$$

where x assumes the physical value of the pressure ratio. Regarding the expander isentropic efficiency, the definition adopted refers to an overall isentropic efficiency which includes also the generator and inverter electro-mechanical losses. The reason is that in the current ORC test rig, the power generated is measured at the inverter. By means of two correlations for the generator electro-mechanical efficiency and the inverter electrical efficiency, the isentropic efficiency of the expander at the shaft can be estimated:

$$\dot{W}_{el,\exp inv} = \varepsilon_{oa,\exp}\dot{W}_{s,\exp} = \varepsilon_{s,sh,\exp}\eta_{el-m,gen}\eta_{el,inv}\dot{W}_{s,\exp} = \eta_{el-m,gen}\eta_{el,inv}\dot{W}_{sh,\exp}. (11)$$

The influence of the electro-mechanical losses at different rotational speeds of the expander have been analysed in [27]. A contour plot of Eq. 10 is shown in Fig. 4. The peak of the overall isentropic efficiency is at a pressure ratio between 6 and 7 for a rotational speed of 3000 rpm.

3.2.4. Liquid receiver and line sets

In the ORC installation, a liquid receiver is placed after the condenser. Normally, the liquid receiver is used to damp possible mass flow rate fluctuations during transient operations and ensures a subcooled state of the fluid entering the pump in order to avoid cavitation. In this case, the liquid receiver has an approximate volume of 50L which cannot be neglected for the charge estimation. A level sensor is installed on top of the tank to monitor the fluctuations of the refrigerant liquid phase. The liquid receiver is considered to be adiabatic and its volume represents the only parameter (pressure drops at inlet/outlet are neglected). The steady-state level of the receiver is given by:

$$level = \left(\frac{h_{r,v,sat} - h_{r,su}}{h_{r,v,sat} - h_{r,l,sat}}\right)\frac{\rho_{r,su}}{\rho_{l,sat}} = \frac{m_{r,l,sat}}{m_{r,tot}}\frac{v_{l,sat}}{v_{r,su}} = \frac{V_l}{V_{tot}}. \quad (12)$$

As outputs, the model calculates the inlet pressure, the liquid level and the refrigerant charge.

The pressure drops and heat losses through the pipeline connections between components are also taken into account. The model includes heat transfer to the environment, internal heat transfer and pressure drop. The overall heat transfer coefficient, UA, is the sum of the thermal resistance of the tube, the thermal resistance associated with the insulation and the convective UA values associated with the inside and outside of the tube. The pressure drops are calculated for single-phase flow. The total volume of the line sets allows to better characterize the refrigerant charge.

4. Parametric study and discussion

The comparison of the low-GWP working fluids with the baseline R245fa is carried out by fixing the inlet conditions of the cold source and cold sink fluids, i.e. temperature, pressure and mass flow rate. In this case, the cold source inlet condition at the condenser is fixed at 20°C and the maximum mass flow rate is assumed, i.e. 4 kg/s. These represent typical testing conditions for the ORC unit considered. The hot source is the thermal oil T66 and two temperatures are investigated (120°C and 90°C), since they are representative of typical low-grade waste heat temperatures. The mass flow rate of T66 is fixed at 3 kg/s. The expander speed is maintained constant at the nominal speed of 3000 rpm. A sweep of the pump rotational speed is performed in the range from 1500 rpm up to 2500 rpm. The choice of this range of operation is consistent with the experimental tests performed with R245fa. Finally, the subcooling has been fixed at 3 K. During operation, the subcooling level changes while it is also related with the total charge of the system. In this case, since the total

charge of the low-GWP working fluids is not known a priori, the subcooling level has been chosen as the average of the experimental values obtained with R245fa. The simulation matrix is summarized in Table 3. The performance of an ORC unit for a given set of boundary conditions strongly depends on the behaviour of the pump and the expander. In the detailed cycle model, the mass flow rate is imposed by the pump as it occurs in a real ORC installation. A comparison between the mass flow rate delivered by the pump and the electrical power required at different pressure ratios is shown in Fig. 5.

Pressure difference across the pump and mass flow rate are linked in a centrifugal pump. The mass flow rate displaced by the pump in the case of R1234ze(Z) and R245fa is comparable throughout the range. However, due to the difference in specific gravity of these two fluids, the maximum pump head achievable with R1234ze(Z) is lower than in the case of R245fa. In fact, at the same temperature condition, R1234ze(Z) presents a slightly higher pressure (see Fig. 3). Vice versa, the pump delivers a lower mass flow rate in the case of R1233zd(E), but with a higher maximum pressure ratio. As stated earlier, R1233zd(E) requires a lower pressure compared to R245fa and R1234ze(Z) at given evaporating temperature. The power consumption follows the trend of the mass flow rates. The isentropic efficiency of the pump ranges between 0.2 and 0.3.

The performance of the expander is compared for two different hot source inlet conditions. In Fig. 6(a), the case at 120°C is shown. The expander power behaves quasi-linear with respect to the pressure ratio, which is comparable to the experimental results. Under the considered conditions, the electrical power output obtained with R1234ze(Z) is higher than for R245fa. However, the difference in net power, i.e. expander power deducted by the pump power, is negligible for R1234ze(Z) and R245fa due to higher pump power requirements of the low-GWP fluid. On the other hand, in the case of R1233zd(E), the expander power output is generally lower, but the net power is also comparable to R245fa. In Fig. 6(b), the case at 90°C is considered. As expected the power output increases at higher pressure ratios until saturated conditions at the expander inlet are reached, i.e. zero superheating. The power output sharply decreases in the case of two-phase expansion, which is out of the scope of this study. Considerations similar to the case at 120°C can be made.

The results obtained are generally in agreement with other studies performed with R1234ze(Z) and R1233zd(E) [8-12]. Simulations suggest that both fluids are suitable candidates to replace of R245fa. Experimental work is required to assess the impact of these fluids on the performance of the expander, in order to optimize a given installation with the new fluids.

Table 3. Running conditions of the ORC.

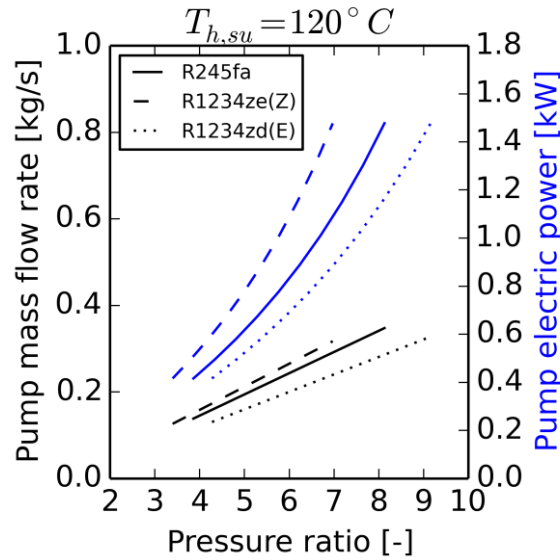| Imposed variables	Values
Hot source fluid	Therminol 66
Hot source inlet temperature, °C	120,90
Hot source mass flow rate, kg/s	3
Cold sink fluid	water+glycol (30% vol.)
Cold sink inlet temperature, °C	20
Cold sink mass flow rate, kg/s	4
Expander speed, rpm	3000
Pump speed, rpm	1500-2500
Subcooling, K	3

Fig. 5. Comparison of the centrifugal pump performance running with R245fa, R1234ze(Z) and R1233zd(E). Mass flow rate and electric power consumption are shown in the graph at different pressure ratios.
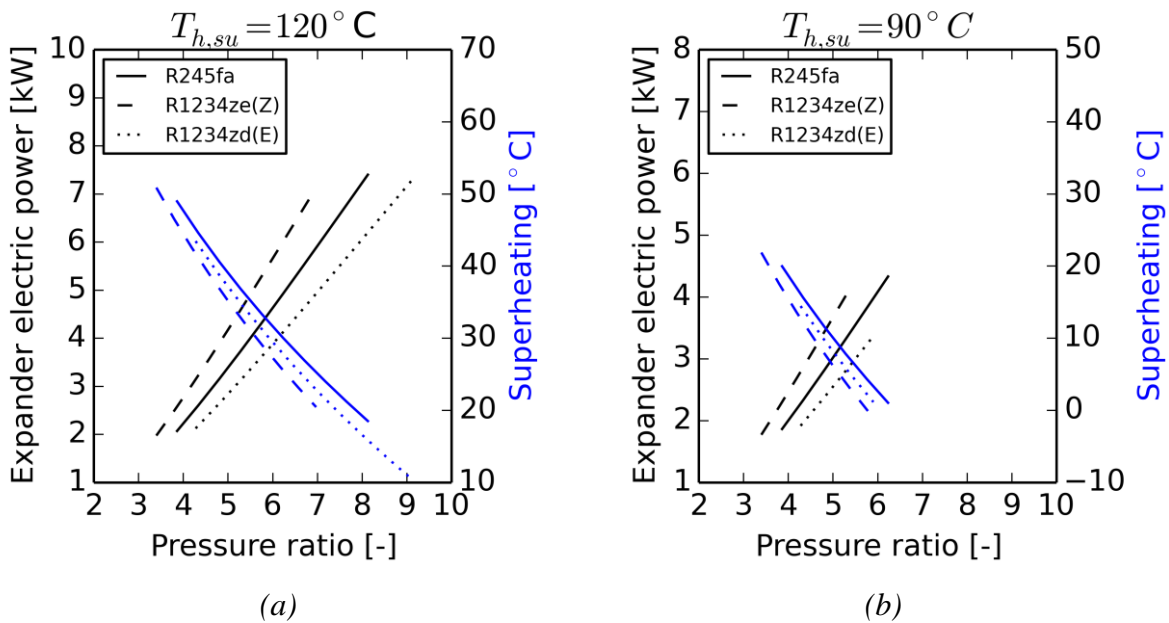

Fig. 6. Comparison of expander electrical power output as function of pressure ratio for two different heat source inlet temperatures (a) 120°C ; (b) 90°C. The superheating level at different pressure ratios is also represented. The condenser inlet temperature of the cooling medium is kept constant at 20°C.

5. Conclusion

In this paper, an open-source ORC modelling library has been introduced with the aim of covering the lack of modelling tools available to enhance the research on ORCs. The library covers three main programming languages used nowadays and it includes models and examples both at component and cycle levels. A detailed simulation model of a regenerative ORC system has been developed and further used to investigate the impact of low-GWP working fluids R1234ze(Z) and R1233zd(E) as drop-in replacements of R245fa currently used in the installation. Based on the thermo-physical properties, the two low-GWP represent good candidates. A parametric study has

been carried out by considering two hot source inlet temperatures, i.e. 90°C and 120°C, at fixed temperature and mass flow rate of the cold source, 20°C and 4 kg/s, respectively. Results show that under the given conditions R1234ze(Z) has a performance comparable to R245fa with a slight increase in power output ranging from 5% to 15%. On the other hand, R1233zd(E) achieved higher net power output (up to 1%) at lower pressure ratios. It is concluded that both fluids are suitable candidates as drop-in replacements of R245fa without significant design changes of a certain ORC unit.

Nomenclature

h	specific enthalpy, J/kg
L	length
$\dot{m}$	mass flow rate, kg/s
N	rotational speed, rpm
p	pressure, Pa
T	temperature, °C
$\dot{Q}$	heat rate, W
r_p	pressure ratio, -
$r_{v,built-in}$	Built-in volume ratio, -
u	specific internal energy, J/kg
v	specific volume, m³/kg
V	Volume, m³
$\dot{V}$	volumetric flow rate, m³/s
w	zone length fraction, -
$\dot{W}$	power, W

Subscripts and superscripts

amb	Ambient
c	cold
calc	calculated
cond	condenser
eq	equivalent
ex	exhaust
g	groove
gen	generator
h	Hot fluid
inv	inverter
l	liquid
p	pump
r	refrigerant
ref	reference
sh	shaft
su	supply
tot	total
v	vapor, volume

Greek symbols

η	efficiency
ρ	density
ε	effectiveness
ϕ_{FF}	filling factor

References

[1] Quoilin S., van den Broek M., Declaye S., Dewallef P., Lemort V., Techno-economic survey of Organic Rankine Cycle (ORC) systems, Renewable and Sustainable Energy Reviews 2013;22:168-186.

[2] Hærvig J., Sørensen K., Condra T.J., Guidelines for optimal selection of working fluid for an organic Rankine cycle in relation to waste heat recovery. Energy 2016;96:592-602.

[3] Lecompte S., Huisseune H., van den Broek M., Vanslambrouck B., De Paepe M., Review of organic Rankine cycle (ORC) architectures for waste heat recovery. Renewable and Sustainable Energy Reviews 2015;47:447-461.

[4] Xu J., Luo X., Chen Y., Mo S., Multi-criteria design optimization and screening of heat exchangers for subcritical ORC. Energy Procedia 2015;75:1639-1645.

[5] Lecompte S., Huisseune H., van den Broek M., De Schampheleire S., De Paepe M., Part load thermo-economic optimization of the Organic Rankine Cycle (ORC) applied to a combined heat and power (CHP) system. Applied Energy 2013; 111:871-881.

[6]   Imran M., Usman M., Park B-S, Lee D-H, Volumetric expanders for low grade heat and waste heat recovery applications. Renewable and Sustainable Energy Reviews 2016;57:1090-1109.

[7]   UNEP – United Nations Environment Programme. Assessment of HCFCs and environmentally sound alternatives, scoping study on alternatives to HCFC refrigerants under high ambient temperature conditions. 2014.

[8]   UNEP – United Nations Environment Programme. Overview of issues related to hydrofluorocarbons and their management. Open-ended Working Group of the Parties to the Montreal Protocol on Substances that Deplete the Ozone Layer. Thirty-fifth meeting, Bangkok, 22-24 April 2015.

[9]   Petr P., Raabe G., Evaluation of R-1234ze(Z) as a drop-in replacement for R-245fa in Organic Rankine Cycles – From thermophysical properties to cycle performance. Energy 2015;93:266-274.

[10]   Fukuda S., Kondou C., Takata N., Koyama, S., Low GWP refrigerants R1234ze(E) and R1234ze(Z) for high temperature heat pumps. International Journal of Refrigeration 2014; 40: 161-173.

[11]   Navarro-Esbri J., Mendoza-Miranda J.M., Mota-Babiloni A., Barragan-Cervera A., Belman-Flores J.M., Experimental analysis of R1234yf as a drop-in replacement for R134a in a vapour compression system. International Journal of Refrigeration 2013; 36:870-880.

[12]   Le V.L., Feidt M., Kheiri A., Pelloux-Prayer S., Performance optimization of low-temperature power generation by supercritical ORCs (organic Rankine cycles) using low GWP (global warming potential) working fluids. Energy 2014;67:513-526.

[13]   Datla B.V., Brasz J.J., Comparing R1233zd and R245fa for Low Temperature ORC Applications. Proceedings of 15th International Refrigeration and Air Conditioning Conference at Purdue, July 14-17,2014. Paper 2546.

[14]   Kontomaris K., HFO-1336mzz-Z: High Temperature Chemical Stability and Use as Working Fluid in Organic Rankine Cycles. 15th International Refrigeration and Air Conditioning Conference at Purdue, 14-17 July 2014. Paper 2550.

[15]   Ziviani D., Woodland B.J., Georges E., Groll E.A., Braun J.E., Horton W.T., De Paepe M., van den Broek M., ORCSIM: a Generalized Organic Rankine Cycle Simulation Tool. Proceedings of 3rd Seminar on ORC Power Systems, October 12-14 2015, Brussels, Belgium. Paper 30.

[16]   Dickes R., Ziviani D., De Paepe M., van den Broek M., Quoilin S., Lemort V., ORCmKit: an open-source library for organic Rankine cycle modeling and analysis. Submitted to 29th ECOS, June 19-23 2016, Portorož, Slovenia.

[17]   Akasaka R., Zhou Y., Lemmon E.W., A fundamental Equation of State for 1,1,1,3,3-Pentafluoropropane (R245fa). Journal of Physical and Chemical Reference Data 2015;44:013104.doi: 10.1063/1.4913493

[18]   Nelson D.D., Zahnsir M.S. Jr., Kolb C.E., Magid H., OH reaction kinetics and atmospheric lifetime estimates for several hydrofluorocarbons. J. Phys. Chem. 1995;99:16301-16306.

[19]   Nilsson E.J.K., Nielsen O.J., Johnson M.S., Hurley M.D., Wallington T.J., Atmospheric chemistry of cis-$CF_3CH=CHF$: Kinetics of reactions with OH radicals and O_3 and products of OH radical initiated oxidation. Chem. Phys. Lett. 2009;473:233-237.

[20]   Sulbaek Andersen M.P., Nielsen O.J., Hurley M.D., Wallington T.J., Atmospheric chemistry of t-$CF_3CH=CHCl$: products and mechanisms of the gas-phase reactions with chlorine atoms and hydroxyl radicals. Phys.Chem.Chem.Phys 2012.14:1735-1748.

[21]   Hulse J.R., Basu R.S., Singh R.R., Thomas R.H.P., Physical Properties of HCFO-1233zd(E). J. Phys. Chem. 2012;57:3581-3586.

[22]   Wuebbles D.J., Wang D., Patten K.O., Olsen S.C., Analyses of new short-lived replacements for HFCs with large GWPs. Geophysical Research letters 2013;40:4767-4771.

[23]   Lemmon E.W., Huber M.I., Mclinden M.O., REFPROP, Reference Fluid Thermodynamic and Transport Properties. NIST standard reference database 23. Version 9.1. 2013. Gaithersburg.

[24] Bell I.H., Quoilin S., Georges E., Braun J.E., Groll, E.A., Horton W.T., Lemort V., A generalized moving-boundary algorithm to predict the heat transfer rate of counterflow heat exchangers for any phase configuration. Applied Thermal Engineering 2015;79(-):192-201.

[25]   Nagata R., Kondou C., Koyama S., Comparative assessment of condensation and pool boiling heat transfer on horizontal plain single tubes for R1234ze(E), R1234ze(Z) and R1233zd(E). International Journal of Refrigeration 2016;63:157-170.

[26]   Ziviani D., Bell I.H., De Paepe M., van den Broek M., Update on single-screw expander geometry model integrated into an open-source simulation tool. IOP Conf. Series: Materials Science and Engineering 2015;90:012064.

[27]   Ziviani D., Desideri A., Lemort V., De Paepe M., van den Broek M., Low-order models of a single-screw expander for organic Rankine cycles applications. IOP Conf. Series: Materials Science and Engineering 2015;90:012061.